Cross-correlation frequency-resolved optical gating coherent anti-Stokes Raman scattering with frequency-converting photonic-crystal fibers

S. O. Konorov,[1] D. A. Akimov,[1,2] E. E. Serebryannikov,[1] A. A. Ivanov,[3] M. V. Alfimov,[3] and A. M. Zheltikov[1,2]
[1]*Physics Department, M.V. Lomonosov Moscow State University, 119899 Moscow, Russia*
[2]*International Laser Center, M.V. Lomonosov Moscow State University, 119899 Moscow, Russia*
[3]*Center of Photochemistry, Russian Academy of Sciences, Novatorov 7a, Moscow 117421, Russia*
(Received 22 April 2004; published 3 November 2004)

Photonic-crystal fibers provide a high efficiency of frequency upconversion of regeneratively amplified femtosecond pulses of a Cr: forsterite laser, permitting the generation of subpicosecond anti-Stokes pulses with a smooth temporal envelope and a linear positive chirp, ideally suited for femtosecond coherent nonlinear spectroscopy. These pulses from a photonic-crystal fiber were cross correlated in our experiments with the femtosecond second-harmonic output of the Cr: forsterite laser in toluene solution, used as a test object, in boxcars geometry to measure the spectra of coherent anti-Stokes Raman scattering (CARS) of toluene molecules (XFROG CARS).

DOI: 10.1103/PhysRevE.70.057601 PACS number(s): 42.65.Wi, 42.79.−e, 42.81.−i

About 30 years ago, nonlinear Raman spectroscopy benefited tremendously from the application of tunable laser sources, such as optical parametric oscillators [1] and dye lasers [2] were demonstrated to greatly simplify measurements using coherent anti-Stokes Raman scattering (CARS), making these measurements much more informative, efficient, and convenient. Broadband laser sources later contributed to the technical and conceptual progress in nonlinear Raman spectroscopy [3–5], allowing single-shot CARS measurements. In the era of femtosecond lasers, several parallel trends have been observed in the development of laser sources for nonlinear Raman spectroscopy [6]. One of these tendencies was to adapt broadband femtosecond pulses for spectroscopic purposes [6–8] and to use different spatial phase-matching geometries to simultaneously generate coherent Stokes and anti-Stokes, as well as degenerate four-wave mixing signals [6,9]. The rapid progress in nonlinear materials, on the other hand, resulted in the renaissance of optical parametric oscillators and amplifiers (OPO's and OPA's) for nonlinear spectroscopy [10]. Chirped pulses [11,12] were used to probe broad spectral regions and large ranges of delay times, suggesting efficient single-shot nonlinear spectroscopic approaches. Here we will show that photonic-crystal fibers (PCF's) [13,14] capable of generating ultrashort frequency-tunable pulses with a controlled chirp through enhanced nonlinear-optical processes [15,16] are ideally suited for nonlinear coherent spectroscopy, offering attractive cost-efficient solutions for the creation of novel compact sources of frequency-tunable chirped ultrashort pulses for nonlinear spectroscopic applications, supplementing in many ways currently available OPA's and dye laser sources.

Photonic-crystal fibers employed in our experiments were fabricated using a standard technology [13,14,17] and were made of S93-1 glass with additions of S95-2 glass. The cross-section view of PCF's used in this work is shown in the inset to Fig. 1. An asterisk-shaped core of the fiber had a diameter of approximately 2 μm.

The laser system employed in our experiments (Fig. 1) consisted of a Cr^{4+}: forsterite master oscillator, a stretcher, an optical isolator, a regenerative amplifier, and a compressor. The master oscillator, pumped with a fiber ytterbium laser, generated 30–50-fs light pulses of radiation with a wavelength of 1.24 μm at a repetition rate of 120 MHz. These pulses were then transmitted through a stretcher and an isolator to be amplified in a Nd: YLF-laser-pumped amplifier and recompressed to the 75–100-fs pulse duration with the maximum laser pulse energy up to 40 μJ at 1 kHz. Submicrojoule Cr: forsterite-laser pulses with an initial duration of about 90 fs coupled into the central core of the PCF resulted in the efficient generation of anti-Stokes signal (Fig. 2) through parametric wave-mixing processes [15–19], with the central wavelength of the anti-Stokes signal dictated by phase matching and controlled by fiber dispersion. The anti-Stokes wavelength can also be finely tuned by changing the intensity of the pump pulse (Fig. 2) due to the nonlinear change in the refractive index of the fiber core and the spectral broadening of the pump pulse.

Cross-correlation frequency-resolved optical gating (XFROG) [20] was used to characterize anti-Stokes pulses generated in the PCF. An XFROG signal was generated by

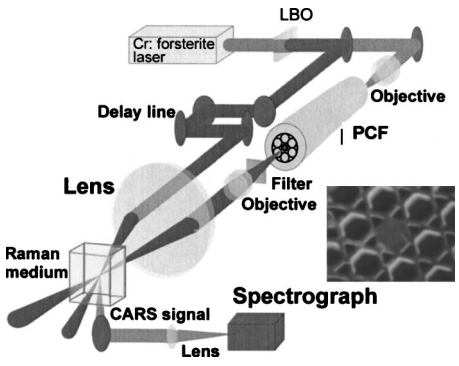

FIG. 1. Diagram of femtosecond CARS spectroscopy with the use of ultrashort pulses frequency-upconverted and chirped in a photonic-crystal fiber. The inset shows the cross-section view of the central part of the photonic-crystal fiber.

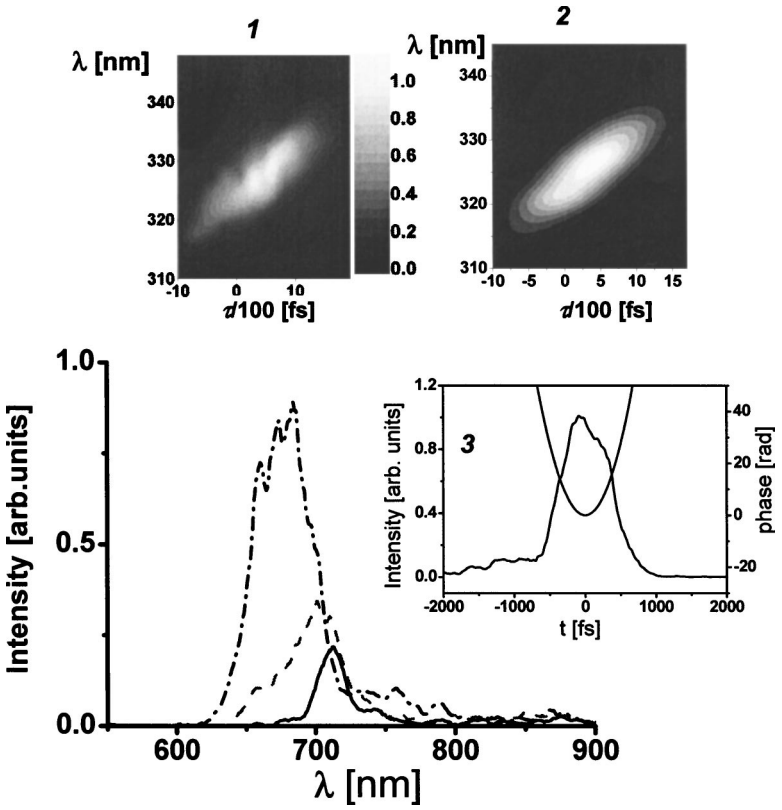

FIG. 2. The spectrum of the anti-Stokes signal generated in a photonic-crystal fiber by 1.24 -μm 90-fs Cr: forsterite-laser pulses with an input energy of (solid line) 170 nJ, (dashed line) 220 nJ, and (dash--dotted line) 270 nJ. The insets show (1) the intensity of the sum-frequency signal generated in a BBO crystal by the second-harmonic pulse from the Cr: forsterite laser and the anti-Stokes pulse from the photonic-crystal fiber as a function of the wavelength and the delay time τ between the second-harmonic and anti-Stokes pulses, (2) theoretical fit of the XFROG trace, and (3) pulse envelope and the phase of the anti-Stokes pulse providing the best fit.

mixing the anti-Stokes signal from the fiber E_a with the 620-nm 90-fs second-harmonic output of the Cr: forsterite laser E_{SH} in a BBO crystal. A two-dimensional XFROG spectrogram $S(\omega,\tau)\propto\left|\int_{-\infty}^{\infty}E_a(t)E_{\mathrm{SH}}(t-\tau)\exp(-i\omega t)dt\right|^2$, was then plotted in a standard way [20] by measuring the XFROG signal as a function of the delay time τ between the second-harmonic and anti-Stokes pulses and spectrally dispersing the XFROG signal. The XFROG spectrogram shown in inset 1 to Fig. 2 visualizes the temporal envelope, the spectrum, and the chirp of the anti-Stokes signal generated in the PCF. A reasonable fit of the experimental XFROG trace was achieved (inset 2 in Fig. 2) with an anti-Stokes pulse having a duration of about 1 ps and a linear positive chirp corresponding to the phase $\varphi(t)=\alpha t^2$ with $\alpha=110\ \mathrm{ps}^{-2}$. The spectrum and the phase φ of the anti-Stokes pulse reconstructed with this procedure are shown in inset 3 in Fig. 2.

The linear chirp defines a simple linear mapping between the instantaneous frequency of the anti-Stokes pulse and the delay time τ, allowing spectral measurements to be performed by varying the delay time between the pump pulses [21]. We used 90-fs second-harmonic pulses of the Cr: forsterite laser (at the frequency ω_1) and the linearly chirped pulses from the PCF (the frequency ω_2) as a biharmonic pump for the CARS spectroscopy of toluene solution. The frequency difference $\omega_1-\omega_2$ was scanned through the frequencies of Raman-active modes of toluene molecules by tuning the delay time between the pump pulses [Fig. 3(a)]. The second-harmonic pulse also served as a probe in our CARS scheme, generating the CARS signal at the frequency $\omega_{\mathrm{CARS}}=2\omega_1-\omega_2$ through the scattering from Raman-active vibrations coherently excited by the pump fields. The light beams with frequencies ω_1 and ω_2 were focused into a cell with toluene solution at a small angle with respect to each other (Fig. 1). The CARS signal generated in the area of beam interaction in this noncoplanar boxcars geometry [3–5] had a form of a sharply directed light beam with a low, phase-matching-controlled angular divergence spatially separated (Fig. 1) from the pump beams. Figure 3(b) presents the map of CARS spectra from the toluene solution measured for different delay times τ between the biharmonic pump pulses. This procedure of measurements, in fact, implements the XFROG technique [20]. However, while FROG-based techniques [20,22,23] are usually employed to characterize ultrashort pulses, our goal here is to probe Raman-active modes of toluene molecules, used as a test object, by means of CARS spectroscopy.

In the case of a positively chirped pulse from the PCF (insets 2, 3 in Fig. 2), small delay times τ correspond to the excitation of low-frequency Raman-active modes [$\tau\approx-200$ fs in Fig. 3(b)]. In particular, the 1004-cm^{-1} Raman mode of toluene is well-resolved in the presented XFROG CARS spectrogram. This mode is excited with the second harmonic of Cr: forsterite-laser radiation and the spectral slice around the wavelength of $\lambda_2\approx661$ nm picked with an appropriate τ [Fig. 3(a)] from the positively chirped pulse frequency-upconverted in the PCF, giving rise to a CARS signal with the wavelength $\lambda_{\mathrm{CARS}}\approx584$ nm. Raman modes with higher frequencies are probed at larger delay times [$\tau\approx100-200$ fs in Fig. 3(b)].

We now quantify these data by fitting the experimental XFROG CARS spectrograms using the result of chirped-pulse CARS theory [21]: $S_{\mathrm{CARS}}(\omega_{\mathrm{CARS}},\tau)=\left|\int A_4(\theta,\tau)\exp(i\Delta\omega\theta)d\theta\right|^2$, where $\Delta\omega=\omega_1-\omega_2$, $A_4(\theta,\tau)\propto B_3(\theta)\int_0^{\infty}\chi(t_1)B_1(\theta-t_1)B_2^{*}(\theta-\tau-t_1)\exp\{i[\Delta\omega_1-\alpha(\theta-\tau$

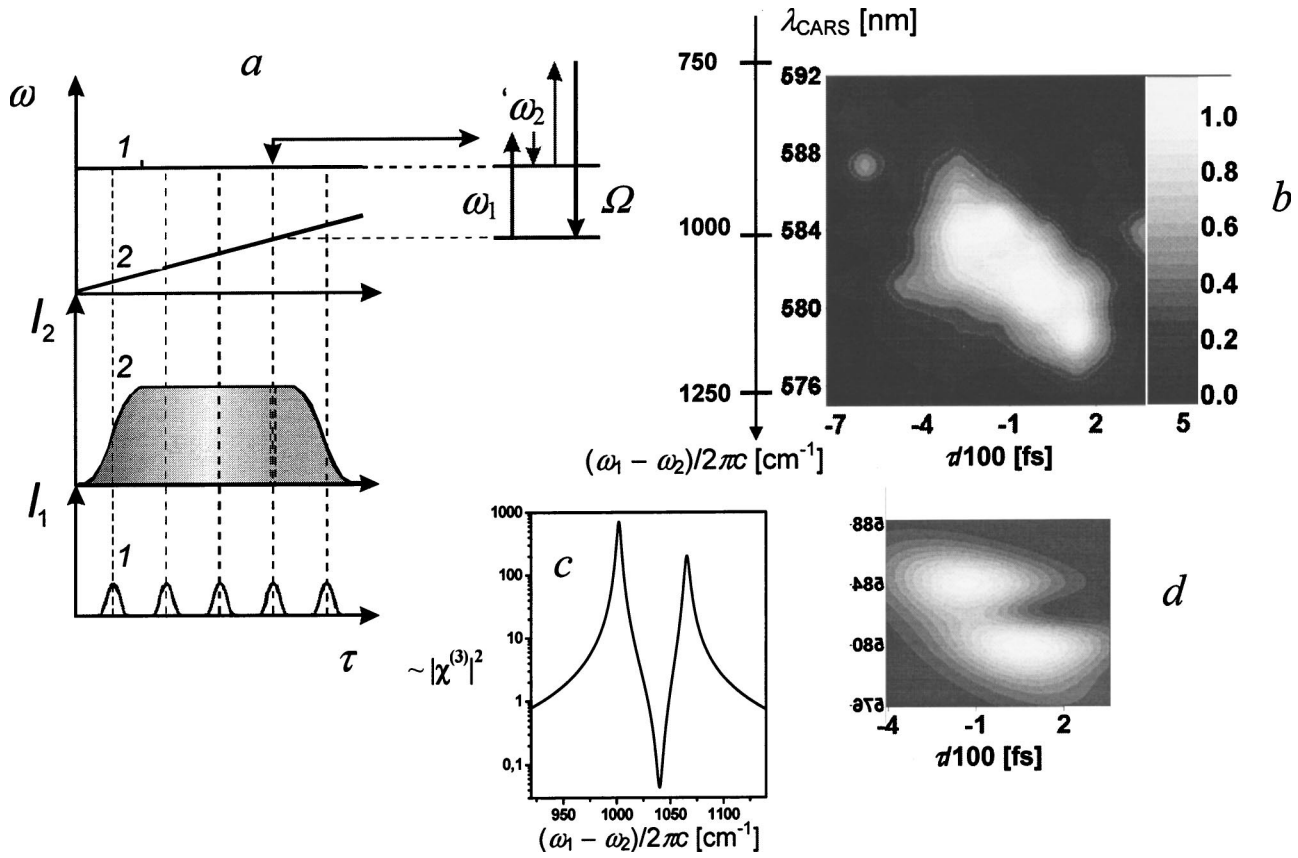

FIG. 3. (a) A diagram of femtosecond CARS spectroscopy with chirped pulses is shown on the left. The first pulse (frequency ω_1) is transform limited. The second pulse (frequency ω_2) is linearly chirped. The linear chirp of the second pulse maps the delay time between the pulses on the frequency, allowing the frequency difference $\omega_1-\omega_2$ to be scanned through Raman resonances Ω by tuning the delay time τ. (b) The intensity of the CARS signal generated in a noncoplanar boxcars geometry from toluene solution as a function of the wavelength and the delay time τ between the second-harmonic and anti-Stokes pulses used as a biharmonic pump. (c) A model of the Raman spectrum, including a doublet of Lorentzian lines and a frequency-independent nonresonant background, used in theoretical fit. (d) Theoretical fit of the XFROG CARS spectrogram.

$-t_1)^2]\}dt_1$, B_j is the envelope of the jth pulse, $\theta=t-z/v$, v is the group velocity, which is assumed to be the same for all the pulses in the cell, $\chi(t_1)$ is the Raman-resonant third-order nonlinear-optical susceptibility, related to the full cubic nonlinear susceptibility $\chi(t_1,t_2,t_3)$, which is a function of three time arguments, by the expression [21] $\chi(t_1,t_2,t_3)=\chi(t_1)\delta(t_1-t_2)\delta(t_3)$.

As a simple model of the Raman spectrum of toluene molecules in the studied spectral range [3], we employ a doublet of Lorentzian lines interfering with the coherent nonresonant background [Fig. 3(c)]. The frequencies of the peaks in these spectra are used as fitting parameters. The ratio of the peak value of the resonant part of the CARS susceptibility $\overline{\chi^{(3)}}$ to the nonresonant susceptibility $\chi_{\mathrm{NR}}^{(3)}$ was estimated by measuring the intensities of the CARS signal on and off the Raman resonances, yielding $|\chi_{\mathrm{NR}}^{(3)}|/|\overline{\chi^{(3)}}|\approx 0.05$. The best fit [Fig. 3(d)] is achieved with the Raman peaks centered at 1004 and 1102 cm^{-1}, which agrees well with earlier CARS studies of toluene [3].

Although the slope of the XFROG CARS trace and positions of Raman peaks can be adequately described with the use of this simple model, some of the spectroscopic features of the experimental XFROG CARS trace deviate from the theoretical fit. These deviations may originate from variations in the coherent background as a function of the frequency. For a quantitative spectroscopic analysis, these inhomogeneities in the frequency dependence of the coherent background should be carefully measured and included in the fit. On the other hand, the nonresonant contribution to CARS spectral profiles can be efficiently suppressed [3,4,6] by using three input pulses in the CARS arrangement instead of two and by introducing the delay time between the third pulse (probe) and the two-color pump, tuned to a Raman resonance under study.

Some of the structure observed in XFROG CARS spectrograms in Fig. 3(b) can also be due to the temporal and spectral structure of the anti-Stokes frequency-upconverted signal generated by the PCF. The XFROG spectrogram of this signal, in fact, suggests the presence of irregular temporal and spatial modulation, which may be due to modulation instabilities and the noise component typical of nonlinear-optical interactions in any PCF. The expressions for the XFROG CARS trace presented above explicitly involve the input fields, showing that the temporal and spectral structure of the anti-Stokes pulse is transferred to the CARS spectro-

gram. For precise quantitative measurements, XFROG CARS traces should be therefore carefully calibrated to include such a structure of one of the input fields in order to avoid distortions, excessive noise, and artifacts in the spectroscopic and time-resolved data retrieved from XFROG CARS spectrograms.

We have shown in this work that photonic-crystal fibers with a specially designed dispersion offer the ways to create efficient sources of ultrashort pulses for coherent nonlinear spectroscopy. These fibers provide a high efficiency of frequency upconversion of regeneratively amplified femtosecond pulses of a Cr: forsterite laser, permitting the generation of subpicosecond linearly chirped anti-Stokes pulses ideally suited for femtosecond coherent nonlinear spectroscopy.

We are grateful to V.I. Beloglazov and N.B. Skibina for fabricating microstructure fibers and to A.B. Fedotov, D.A. Sidorov-Biryukov, and V.P. Mitrokhin for useful discussions. This study was supported in part by the President of Russian Federation Grant No. MD-42.2003.02, the Russian Foundation for Basic Research (Projects Nos. 03-02-16929, 02-02-17098, 04-02-81036-Bel2004-a, and 03-02-20002-BNTS-a), and INTAS (Projects Nos. 03-51-5037 and 03-51-5288). The research described in this publication was made possible in part by Grant No. RP2-2558 of the U.S. Civilian Research & Development Foundation for the Independent States of the Former Soviet Union (CRDF). This material is also based upon the work supported by the European Research Office of the US Army under Contract No. 62558-04-P-6043.

[1] S.A. Akhmanov, V.G. Dmitriev, A.I. Kovrigin, N.I. Koroteev, V.G. Tunkin, and A.I. Kholodnykh, JETP Lett. **15**, 425 (1972).
[2] M.D. Levenson, C. Flytzanis, and N. Bloembergen, Phys. Rev. B **6**, 3962 (1972).
[3] S.A. Akhmanov and N.I. Koroteev, *Methods of Nonlinear Optics in Light Scattering Spectroscopy* (Nauka, Moscow, 1981) (in Russian).
[4] G.L. Eesley, *Coherent Raman Spectroscopy* (Pergamon, Oxford, 1981).
[5] A.C. Eckbreth, *Laser Diagnostics for Combustion Temperature and Species* (Abacus, Cambridge, MA, 1988).
[6] *Femtosecond Coherent Raman Spectroscopy*, edited by W. Kiefer Special Issue of J. Raman Spectrosc. 31, No. 1/2 (2000).
[7] R. Leonhardt, W. Holzapfel, W. Zinth, and W. Kaiser, Chem. Phys. Lett. **133**, 373 (1987).
[8] M. Motzkus, S. Pedersen, and A.H. Zewail, J. Phys. Chem. **100**, 5620 (1996).
[9] M. Schmitt, G. Knopp, A. Materny, and W. Kiefer, Chem. Phys. Lett. **280**, 339 (1997).
[10] D. Brüggemann, J. Hertzberg, B. Wies, Y. Waschke, R. Noll, K.-F. Knoche, and G. Herziger, Appl. Phys. B: Photophys. Laser Chem. **55**, 378 (1992).
[11] E.T. J. Nibbering, D.A. Wiersma, and K. Duppen, Phys. Rev. Lett. **68**, 514 (1992).
[12] T. Lang and M. Motzkus, J. Opt. Soc. Am. B **19**, 340 (2002).
[13] J.C. Knight, J. Broeng, T.A. Birks, and P.St.J. Russell, Science **282**, 1476 (1998).
[14] P.St.J. Russell, Science **299**, 358 (2003).
[15] D.A. Akimov, E.E. Serebryannikov, A.M. Zheltikov, M. Schmitt, R. Maksimenka, W. Kiefer, K.V. Dukel'skii, V.S. Shevandin, and Yu.N. Kondrat'ev, Opt. Lett. **28**, 1948 (2003).
[16] S.O. Konorov and A.M. Zheltikov, Opt. Express **11**, 2440 (2003).
[17] A.N. Naumov, A.B. Fedotov, A.M. Zheltikov, V.V. Yakovlev, L.A. Mel'nikov, V.I. Beloglazov, N.B. Skibina, and A.V. Shcherbakov, J. Opt. Soc. Am. B **19**, 2183 (2002).
[18] S. Coen, A. Hing Lun Chau, R. Leonhardt, J.D. Harvey, J.C. Knight, W.J. Wadsworth, and P.St.J. Russell, J. Opt. Soc. Am. B **19**, 753 (2002).
[19] J.M. Dudley, L. Provino, N. Grossard, H. Maillotte, R.S. Windeler, B.J. Eggleton, and S. Coen, J. Opt. Soc. Am. B **19**, 765 (2002).
[20] J.M. Dudley, X. Gu, L. Xu, M. Kimmel, E. Zeek, P. O'Shea, R. Trebino, S. Coen, and R.S. Windeler, Opt. Express **10**, 1215 (2002).
[21] A.N. Naumov and A.M. Zheltikov, Appl. Phys. B: Lasers Opt. **77**, 369 (2003).
[22] R. Trebino, *Frequency-Resolved Optical Gating: The Measurement of Ultrashort Laser Pulses* (Kluwer Academic Publishers, Boston, 2002).
[23] P.-A. Lacourt, J.M. Dudley, J.-M. Merolla, H. Porte, J.-P. Goedgebuer, and W.T. Rhodes, Opt. Lett. **27**, 863 (2002).